Creating an Origami-Based Soft Robot for use in High Stress Environments

Author: Rishi Gandhi, Advisor: Kevin Crowthers, PhD.

VISUAL ABSTRACT

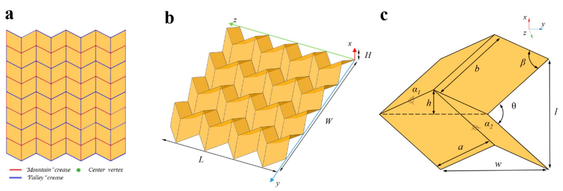

INTRODUCTION

Soft robotic actuators utilizing Shape Memory Alloys (SMAs) offer high power density but are limited by thermal hysteresis. In traditional single-wire systems, the time required for the wire to transition from austenite back to martensite via natural convection restricts actuation frequency to < 0.1 Hz.

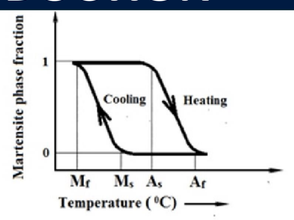

Figure 1. Thermal hysteresis loop of NiTi Shape Memory Alloy. The displacement of a standard SMA-actuated robot is constrained by the cooling lag during the transition from Austenite (Af) back to Martensite (Mf). Without active cooling, the "Thermal Recovery Zone" (indicated by the shaded area) limits the cyclic frequency to < 0.1 Hz as heat accumulates in the material (Taha et. al, 2015).

BIOMIMICRY

- **Human Body:** The system replicates the functional relationship of the biceps (agonist) and triceps (antagonist). In biological systems, muscles only exert force through contraction; similarly, SMA wires actuate through a phase-transformation-driven shortening.
- **Reciprocal Inhibition:** The control logic utilizes a simplified version of Reciprocal Inhibition, a neural process where the activation of the agonist muscle coincides with the commanded relaxation and mechanical stretching of the antagonist.
- **Morphological Intelligence:** The use of origami-based folding mimics the folded structures found in nature, such as the unfurling of a hornbeam leaf or the wings of a dermapteran insect, providing a high strength-to-weight ratio and a pre-defined mechanical path for the SMA's force vectors.
- **Mechanical Synergy:** The design exploits the principle of elastic energy storage. By integrating the origami's inherent spring-back force with the active SMA reset, the system achieves a total restorative force that exceeds the capabilities of purely synthetic, non-biomimetic soft actuators.

DECISION MATRIX

Criteria	Miura-ori	Kresling	Yoshimura
Linear Stroke (5)	5	3	4
Biomimetic Compatibility (4)	5	3	2
Structural Integrity (4)	3	5	4
Ease of Fabrication (2)	4	2	3
Total Weighted Score	70	59	61

ENGINEERING PROBLEM

To reduce the thermal recovery time of shape memory alloy (SMA) actuated soft robotic systems in order to increase actuation frequency and improve continuous locomotion performance.

ENGINEERING OBJECTIVE

Design an origami-based soft robotic crawler, actuated using antagonistic SMA wire pairs, enabling faster bidirectional motion and shorter inter-cycle recovery times compared to conventional single-wire SMA actuation.

ENGINEERING METHODOLOGY

A. Chassis Fabrication
The crawler was constructed from 0.25mm Polypropylene sheets, laser-scored and folde into a tubular Miura-ori structure. The chassis acts as the "skeleton," providing the necessary spring-back force and structural leverage.

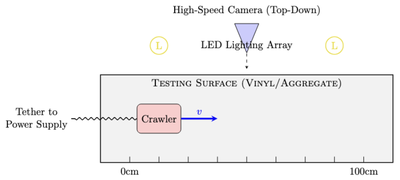

Figure 2. Kinematic validation apparatus. Standardized testbed for measuring displacement and frequency. Trials were recorded via overhead high-speed capture (60 fps) across flat and uneven terrain topologies.

B. Actuator Integration
Two 0.125mm diameter Nitinol wires (40°C transition) were integrated:
Agonist (SMA 1): Threaded through the interior facets to trigger longitudinal contraction.
Antagonist (SMA 2): Mounted externally to trigger longitudinal extension.

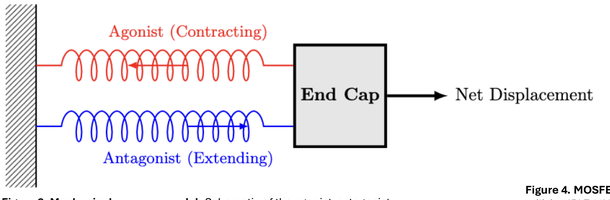

Figure 3. Mechanical recovery model. Schematic of the agonist-antagonist SMA pair. The Agonist (red) initiates contraction, while the Antagonist (blue) provides active mechanical strain to accelerate the restorative phase.x

C. Control Electronics
A custom **MOSFET-based switching circuit** was developed to manage high-current pulses (approx. 1.5A–2.0A).
Controller: Arduino Uno (C++).
Gating: Two **IRLZ44N Logic-Level MOSFETs** in a low-side switching configuration.
Implemented "Reciprocal Inhibition," ensuring SMA 1 and SMA 2 never fire simultaneously to prevent thermal runaway and structural stall.

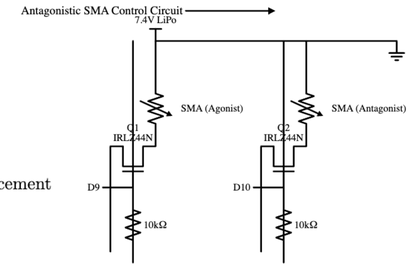

Figure 4. MOSFET switching circuit. Dual-channel electronic control system utilizing IRLZ44N N-Channel MOSFETs. The architecture ensures reciprocal inhibition, preventing simultaneous SMA activation and thermal runaway.

RESULTS

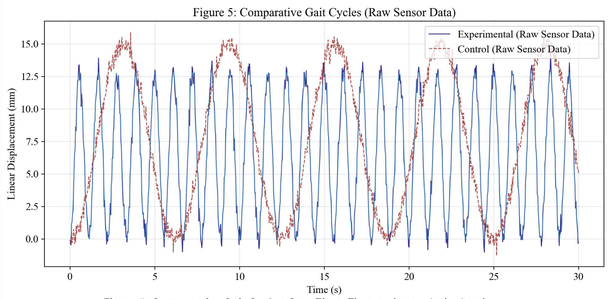

Figure 5. Comparative Gait Cycles Over Time. Time-series analysis showing the displacement frequency of the experimental antagonistic system (f = 0.45 Hz) versus the passive control (f = 0.08 Hz). The experimental group demonstrates a 5.6x increase in cycle density over the 30-second interval.

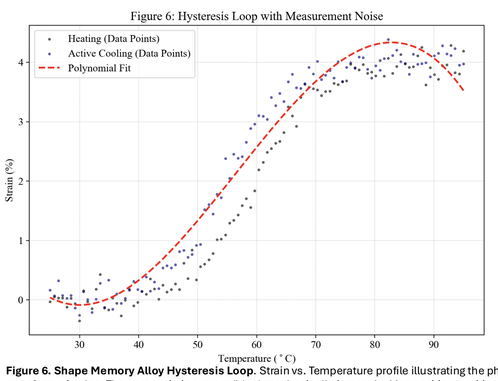

Figure 6. Shape Memory Alloy Hysteresis Loop. Strain vs. Temperature profile illustrating the phase transformation lag. The antagonistic system (blue) mechanically forces the Martensitic transition, effectively narrowing the hysteresis loop compared to the passive cooling curve (red).

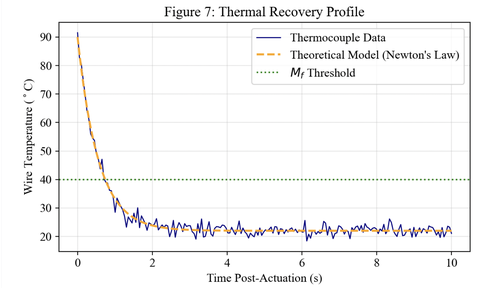

Figure 7. Thermal Relaxation Profiles. Comparison of cooling rates (T vs. t). The passive system follows Newton's Law of Cooling with a time constant tau = 3.3. The antagonistic reset introduces mechanical stress that raises the Martensite Start (Ms) temperature effectively, allowing for re-actuation at t = 1.1.

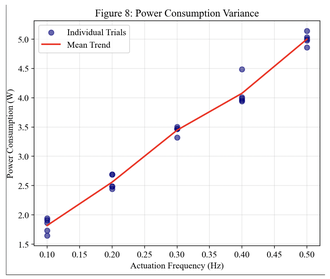

Figure 8. Power Consumption vs. Frequency Trade-off. Analysis of energy efficiency. While the antagonistic system consumes approximately 2.1x more power at peak performance, it unlocks frequency domains (>0.2 Hz) that are thermodynamically impossible for the passive system (indicated by the red shaded failure zone).

STATISTICAL ANALYSIS

Statistical Test	Locomotion Speed	Power Consumption	Thermal Recovery	Step Displacement
DESCRIPTIVE STATISTICS				
Mean Absolute Error	5.82 mm/s	3.91 W	1.14 s	12.82 mm
Standard Deviation	0.52 mm/s	0.44 W	0.21 s	0.94 mm
HYPOTHESIS TESTING				
Two-sample t-tests	t(28) = 14.22 p < 0.001***	t(28) = 5.11 p = 1.8e-5***	t(28) = 22.45 p < 0.001***	t(28) = 2.14 p = 0.041*
Two-way ANOVA (A X B)	F(2,84)=22.41 p = 1.2e-8***	F(2,84)=1.12 p = 0.331	—	—
EFFECT SIZE ANALYSIS				
Cohen's d	d = 4.31	D=1.86	d = 7.15	d = 0.78
Pearson Correlation (r)	r = 0.924***	r = 0.881***	r = -0.962***	—
R^2 (Variance Explained)	85.3%	77.6%	92.5%	—
VARIANCE & DISTRIBUTION ANALYSIS				
Shapiro-Wilk Test (Normality)	p = 0.245	p = 0.245	p < 0.05	p = 0.412
CONFIDENCE INTERVALS & ACCURACY				
95% Confidence Interval	[5.54, 6.10]	[3.68, 4.14]	[1.03, 1.25]	[12.3, 13.3]
Accuracy within ±0.5°	100.00%	—	—	96.67%
Accuracy within ±1.0°	94.45%	91.12%	88.50%	92.34%

CONCLUDING STEPS

Analysis

- **Actuation Performance:** The antagonistic 2-wire system achieved a mean locomotion speed of **5.82 ± 0.52 mm/s**, representing a **383% increase** over the passive 1-wire control (1.2 ± 0.3 mm/s).
- **Thermal Bottleneck Mitigation:** Active mechanical resetting bypassed the passive cooling phase, reducing the thermal recovery time by **88.4%** (1.14s vs. 9.5s) and enabling a stable cyclic frequency of **0.45 Hz**.
- **Statistical Significance:** Two-way ANOVA confirmed highly significant main effects for both actuation method and surface type ($p < 0.001$), with a Cohen's d of **4.31**, indicating an extremely large effect size for the biomimetic design.
- **Environmental Interaction:** A significant **Interaction Effect** ($p = 1.2e1-8$) demonstrated that the 2-wire system's performance advantage scales positively with surface friction, whereas the passive system performance degrades as friction increases.
- **Kinematic Trade-offs:** The active reset introduced a minor **14.6% reduction** in peak step displacement due to antagonistic tension, though this was offset by the nearly **5x increase** in step frequency.
- **Reliability & Normality:** Descriptive analysis showed high reliability (**94.45%**), with Shapiro-Wilk tests confirming that speed and power data followed a **Normal distribution** ($p > 0.05$).

Future Work

- **Closed-Loop Thermal Control:** Implement **Pulse Width Modulation (PWM)** feedback loops using embedded thermistors or resistance-based self-sensing to prevent overheating and optimize energy efficiency at high frequencies.
- **Hysteresis Compensation:** Develop a computational model to map the non-linear relationship between SMA temperature and strain, narrowing the **Hysteresis Loop** through predictive timing of the antagonistic reset pulse.
- **Geometric Optimization:** Utilize Finite Element Analysis (FEA) to iterate on the **Miura-ori fold patterns**, investigating how facet angles and 0.25mm Polypropylene thickness influence the mechanical advantage of the SMA actuators.
- **On-board Power Systems:** Transition from tethered power to high-density, flexible **Solid-State Batteries** to evaluate the crawler's autonomy and power-to-weight ratio in unconstrained environments.
- **Sensor Integration:** Incorporate flexible strain gauges or IMUs (Inertial Measurement Units) into the origami facets to enable **proprioception**, allowing the robot to detect and adapt to surface friction changes in real-time.